Effect of Entropy Generation on the Performance of Humidification-Dehumidification Desalination Cycles

Karan H. Mistry[a], John H. Lienhard V[a,*], Syed M. Zubair[b]

[a]*Department of Mechanical Engineering, Massachusetts Institute of Technology, Cambridge, USA*
[b]*Department of Mechanical Engineering, King Fahd University of Petroleum and Minerals, Dhahran, Saudi Arabia*

Abstract

This paper applies irreversibility analysis to characterize humidification-dehumidification (HD) desalination cycles and to identify how to further improve cycles and components. It is shown that minimizing specific entropy generation of the cycle maximizes the gained output ratio (GOR). It is also shown that each cycle has one limiting component that cannot be substantially improved and a second component that should be the target of efforts to minimize entropy generation. Finally, the failure of exergy analysis to yield conclusive results for on-design HD cycle analysis is discussed briefly.

Keywords: humidification-dehumidification, desalination, Second Law analysis, entropy generation, irreversibility analysis, exergy analysis, cycle analysis, cycle optimization

*Corresponding author
Email address: lienhard@mit.edu (John H. Lienhard V)

Nomenclature

Symbols

c_p	specific heat capacity at constant pressure[kJ/kg-K]
$\bar{g}$	molar Gibbs free energy [kJ/kmol]
GOR	gained output ratio [-]
$\dot{H}, h$	enthalpy flow rate, specific enthalpy (per kg dry air for moist air, per kg water for liquid water) [kW, kJ/kg]
h_{fg}	heat of vaporization [kJ/kg]
L	length of heater [m]
$\dot{m}$	mass flow rate [kg/s]
m_r	mass flow rate ratio (seawater to dry air) [-]
MW	molecular weight [kg/kmol]
$\dot{n}_i$	molar flow rate of species i [mol/s]
$\dot{Q}_{in}, \dot{Q}_{sep}$	heat input, heat of separation [kW]
R	specific gas constant [kJ/kg-K]
R_p	recovery ratio [-]
s	specific entropy (per kg dry air for moist air, per kg water for liquid water) [kJ/kg-K]
$\dot{S}_{gen}$	entropy generation rate [kW/K]
s_{gen}	specific entropy generation (per kg product) [kJ/kg-K]
T	temperature [K]
ΔT	temperature difference from heater surface to fluid bulk temperature [K]
$\dot{W}_{least}$	least work of separation [kW]
$\bar{x}$	property of mixture, per mol
$\bar{x}_i$	partial molar property of species i

Greek

ϵ	component effectiveness [-]
η	mole ratio of salt in seawater [-]
η_{II}	Second Law/exergetic efficiency [-]
ω	humidity ratio, mass basis [kg water vapor/kg dry air]
$\bar{\omega}$	humidity ratio, mole basis [mol water vapor/mol dry air]
$\dot{\Xi}$, ξ	exergy flow rate, specific exergy (per kg dry air for moist air, per kg water for liquid water) [kW, kJ/kg]

Subscripts

0	dead state
1–9	system states (see Fig. 1)
a	dry air, air stream
b	bulk property
D	dehumidifier
d	destroyed
f	saturated liquid

h	fluid in heater
H	humidifier, Hot
HT	heater
i, $ideal$	terminal temperature difference of zero
in	inlet
out	outlet
p	product/condensate
$total$	sum of all components
$trans$	transferred
w	seawater, water stream
$wall$	heated surface
WB	wet-bulb

1. Introduction

A fundamental problem with most desalination technologies, including reverse osmosis (RO), multi-stage flash (MSF), and multi-effect distillation (MED), is that they are very energy intensive. RO requires a steady supply of electricity, and both MSF and MED require substantial heat input, usually as steam supplied by a neighboring power plant. In the developing world, the high cost of energy required for traditional desalination methods helps to make these technologies infeasible. Conversely, many areas that suffer from water scarcity have high levels of solar insolation, which suggests that solar powered desalination would be very beneficial to the developing world since the sun provides an abundance of "free" energy.

Humidification-dehumidification (HD) desalination is a fairly simple technology that mimics nature's water cycle and has the potential to operate with solar heating. A solar still is the most basic form of HD in which the water is evaporated through solar heat and then condensed on a cooler surface. Stills prove to be very inefficient since the latent heat of vaporization is immediately lost in the condensation process [1]. By separating the evaporation and condensation processes and by incorporating regenerative heating of the feedwater in the condenser, most of this energy can be recaptured, thus improving the efficiency of the system. This is the basis of HD desalination cycles. Due to the straight-forward design of the process and the potential for production of potable water in remote areas without the need for electricity, HD has received considerable attention over the past few years [1–3].

Surprisingly, few systematic efforts have been made to find the best HD cycles or to improve and optimize existing cycles. Narayan et al. [4] performed a detailed study based on First Law principles in order to identify the optimal configurations for HD cycles. Since the authors are not aware of any comprehensive Second Law analyses of HD cycles, the present paper provides a Second Law analysis of the some of the

better performing cycles identified by Narayan et al. [4]. The goals of this paper are: to show that minimizing the specific entropy generation of the cycle maximizes the gained output ratio (GOR); to explain how irreversibility analysis can help a designer optimize HD cycles; and to illustrate why exergy analysis and Second Law efficiency lead to inconclusive results for HD cycles.

2. HD Closed Air, Open Water Cycles

One of the most basic HD cycles is the closed air, open water (CAOW) cycle. This cycle consists of three components: a humidifier, a dehumidifier, and a heater. Closed air, open water cycles can be divided into two general classes depending upon which stream (air or water) is heated. A prior study [4] showed that CAOW cycles outperform open air, open water cycles and any of the closed water cycles.

Figure 1 is a simple block diagram of the basic CAOW with both a water and an air heater. While a heater can be placed in both fluid streams, typically only one heater is used forming either a water or an air heated cycle.

[Figure 1 about here.]

2.1. Water Heated Cycle

When the heater in Fig. 1 is in the water stream, the cycle forms a closed air, open water, water heated (CAOW-WH) system. The inner stream is the closed stream of humid air. Cold, saturated air exits the dehumidifier at point 1 and then enters the humidifier at point 2. In the humidifier, the moist air increases in temperature and moisture content, exiting the humidifier at point 3, ideally in a saturated state at higher temperature. Finally, the warm, moist air enters the dehumidifier and much of the moisture content is condensed as product water. The air stream is cooled back to point 1. The condensed water is removed from the dehumidifier at point 9.

The outer stream is the water stream. Cold seawater enters the system through the dehumidifier at point 5 and is heated as the moist air condenses. The warmer water is then further heated as it goes from point 6 to 7 in the heater. The hot water is then sent through the humidifier where it heats and moistens the air stream. Finally, the brine is rejected from the system at point 8.

When heating the water in a CAOW cycle, the logical placement for the heater is between the dehumidifier and the humidifier. Heating the water prior to entering the condenser would only serve to raise the cycle's bottom temperature, which would reduce the performance of the system.

2.2. Air Heated Cycle

The closed air, open water, air heated (CAOW-AH) cycle is formed when only the air heater in Fig. 1 is selected. Both the air and the water streams follow the same flow path through the humidifier and dehumidifier, as with the CAOW-WH cycle. However, instead of heating the water stream, the heater is now placed in the air stream. There are two possible locations in the air stream for the heater: before the humidifier and before the dehumidifier.

When the heater is placed prior to the humidifier, hot unsaturated air enters the humidifier at point 2. Hot air can hold a higher moisture content and should result in a more efficient humidification process. When the heater is placed prior to the dehumidifier, hot unsaturated air enters the dehumidifier at the system top temperature resulting in a higher water exit temperature. This warmer water then enters the humidifier and is used to humidify the air.

The second placement results in a much more efficient heating process. A thought experiment can be used to explain this (numerical analysis can be found in [4]). When the humid air is heated before the dehumidifier, most of the transferred energy goes into the water stream (energy recovery). Next, in the humidifier, there is a large temperature

difference (air at point 2 is relatively cold, water at point 7 is quite warm) and a large concentration difference. The temperature and concentration differences result in both heat and mass transfer from the water stream to the air stream. If the heater is placed prior to the humidifier, air at point 2 is hotter than the water and heat transfer occurs in the opposite direction of mass transfer. Since the driving forces of heat and mass transfer compete, a lower performance results. Therefore it is natural to expect that the second placement is better than the first placement.

2.3. Dual Heated Cycle

When both heaters in Fig. 1 are present, the cycle is a closed air, open water, dual heated cycle. The performance of this class of cycles was found to be between that of the AH and WH cycles. Therefore, they are not presented in this paper.

3. Performance Parameters

There are several ways to characterize the performance of HD systems. Some important parameters are defined below.

3.1. Gained Output Ratio

The gained output ratio (GOR), sometimes known as the performance ratio, is a non-dimensional measure of the amount of product produced for a given heat input. Here, it is defined as:

$$\mathrm{GOR} \equiv \frac{\dot{m}_p h_{fg}}{\dot{Q}_{in}} \tag{1}$$

where h_{fg} is the heat of vaporization at the dead state (ambient conditions).

A GOR of 1 means that the system requires enough heat input to directly vaporize all of the produced water and that there is no energy recovery. A basic solar still will have a GOR of approximately 1, if not less owing to losses. A high GOR is desirable

since it means that less heat input is required per unit water produced. When the heat source is a fossil fuel, higher GOR means lower fuel costs. When the heat source is solar radiation, higher GOR means smaller solar collector area.

3.2. Specific Entropy Generation

Specific entropy generation for the cycle is defined as the total entropy generated in each of the components divided by the mass flow rate of product water.

$$s_{gen,total} = \frac{\dot{S}_{gen,total}}{\dot{m}_p} \tag{2}$$

Thermodynamic arguments for the use of this parameter in analysis of HD cycles, based on the least work of separation, are provided in the appendix.

3.3. Second Law/Exergetic Efficiency

Unlike First Law efficiency which measures how much of an energy source is being put to use, Second Law efficiency measures the irreversibilities in a system. A completely reversible system will have a Second Law efficiency of 1 even though the First Law efficiency will be limited to the lower Carnot efficiency. There are various conventions for defining Second Law efficiency; however, a widely used definition that bounds the efficiency between 0 and 1 is that of Bejan and others [5–7]:

$$\eta_{II} = \frac{\dot{\Xi}_{out}}{\dot{\Xi}_{in}} = 1 - \frac{\dot{\Xi}_d}{\dot{\Xi}_{in}} \tag{3}$$

where $\dot{\Xi}$ is total exergy flow rate in or out of the system and $\dot{\Xi}_d$ is total exergy destruction rate.

Second Law efficiency calculations are common for power production cycles as well as various kinds of thermal pumps. However, its use in desalination systems is less

common. Since one would expect a less irreversible system to have better performance, the use of η_{II} as a performance parameter for desalination is discussed in detail below.

4. System and Component Models

4.1. Approximations

All calculations are performed for steady state at atmospheric pressure. Kinetic and potential energy effects are neglected and pumping power is assumed to be negligible compared to heat input.

Seawater properties are approximated by pure water properties. General cooling tower design practice shows that properties, such as the vapor pressure, vary by about 1% per 10,000 ppm salinity [8–10]. Calculations showed that the change in peak GOR, when using 35,000 ppm seawater properties, is less than 8% while all of the general trends remained unchanged. Use of pure water properties and the associated error is acceptable since the purpose of this study is to characterize and better understand the behavior of CAOW cycles. While the slight change in properties will change the magnitudes of the results, the general trends and conclusions are not affected.

The humidifier and dehumidifier are both treated as adiabatic, and it is assumed that the exit moist air from both components is saturated. Bulk temperature of the condensate from the dehumidifier is calculated as a function of the inlet and outlet wet-bulb temperatures.

4.2. CAOW Cycles

Each of the CAOW cycles studied in this paper is pieced together by appropriately connecting the humidifier, dehumidifier, and air or water heater. The mass balances throughout the system remain constant regardless of the heater placement within the cycle.

4.2.1. Mass Balances

The mass balances in each of the components are straightforward, and expressions for each of the mass flow rates can be determined independently of the energy and entropy equations.

Dry Air. Since the cycles in question are closed air cycle, $\dot{m}_a = \dot{m}_1 = \dot{m}_2 = \dot{m}_3 = \dot{m}_4$.

Water. Mass balances on the water stream in the dehumidifier and water heater yield $\dot{m}_w = \dot{m}_5 = \dot{m}_6 = \dot{m}_7$. A mass balance on the water vapor in the dehumidifier air stream gives the mass flow rate of product:

$$\dot{m}_p = \dot{m}_9 = \dot{m}_a \left(\omega_4 - \omega_1\right) \tag{4}$$

Finally, a water mass balance in the humidifier shows that

$$\dot{m}_b = \dot{m}_8 = \dot{m}_w - \dot{m}_p \tag{5}$$

For convenience, the mass flow rate ratio is introduced:

$$m_r \equiv \frac{\dot{m}_w}{\dot{m}_a} \tag{6}$$

Either two mass flow rates or one mass flow rate and the mass flow rate ratio need to be arbitrarily selected in order to fully define the mass balances.

4.3. Component Governing Equations

For the basic cycle, seven states require specification of pressure, temperature, and relative humidity (for moist air stream). Based on the above approximations, pressures, relative humidities, and condensate temperature are assumed to be given in the calculations that follow. Therefore, the only unknowns in the system are temperatures

at six states. The seawater inlet temperature is fixed and the system top temperature is treated as an input which means only four temperatures are left unknown in the analysis. Energy and entropy balances for the humidifier and dehumidifier provide four equations but introduce two unknown entropy generation terms. In order to solve the cycle, two additional equations must be used. These are equations for the adiabatic heat and mass exchanger effectiveness.

Note that while First and Second Law equations are written for the heater as well, the heater is already well posed and does not add to the complexity of the model.

An exergy balance is also calculated for each component and for the cycle as a whole after all cycle states have been determined.

4.3.1. Exchanger Effectiveness

The effectiveness of the humidifier and dehumidifier is calculated in a similar fashion as effectiveness is calculated for a two stream heat exchanger. In the latter case, effectiveness is defined as the actual heat transfer divided by the theoretical maximum heat transfer, $C_{min}\,(T_{hot,in} - T_{cold,in})$, where C_{min} is the minimum heat capacity rate of the two streams. The mass transfer between the air and water streams in the present case makes the stream enthalpy change, as a function of temperature and humidity, the natural variable upon which to focus. Therefore, an alternate method of calculating the effectiveness is formulated [11, 12]. First, the effectiveness is calculated in two ways — assuming the water stream has the lower maximum enthalpy change, ϵ_w, and then assuming the air stream has the lower maximum enthalpy change, ϵ_a:

$$\epsilon_w = \frac{\Delta \dot{H}_w}{\Delta \dot{H}_{w,ideal}} \qquad \epsilon_a = \frac{\Delta \dot{H}_a}{\Delta \dot{H}_{a,ideal}} \tag{7a}$$

The two ideal enthalpy changes are evaluated assuming a zero terminal temperature difference at the top (or bottom) of the exchanger: $T_{w,out,ideal} = T_{a,in}$ and $T_{a,out,ideal} =$

$T_{w,in}$. Additionally, the moist air stream is assumed to be saturated ($\phi = 1$) at the exits.

Note that the numerators of Eq. (7a) are equivalent for adiabatic exchangers by the First Law. Additionally, the stream with the lower total capacity will have a smaller ideal enthalpy change. Therefore, the actual effectiveness will always be the greater of these two values. Therefore, the effectiveness, ϵ is found by taking the maximum of the two values.

$$\epsilon = \max\left(\epsilon_w, \epsilon_a\right) \tag{7b}$$

Based on this definition of the component effectiveness, it is important to note that it is not always possible to achieve one hundred percent effectiveness without producing temperature cross overs between the streams, which would violate the Second Law. This is similar to the inability of parallel flow heat exchangers to reach one hundred percent effectiveness for some capacity rate ratios, as discussed in more detail in [11, 12]. All calculations were verified in order to ensure that entropy generation was always greater than zero.

4.3.2. Dehumidifier

The dehumidifier is a two phase, two stream heat exchanger in which the water vapor in the air stream condenses on a surface that is cooled by the water stream. The governing equations are:

First Law.

$$0 = \underbrace{\dot{m}_w\left(h_5 - h_6\right)}_{\Delta\dot{H}_{D,w}} + \underbrace{\dot{m}_a\left(h_4 - h_1\right) - \dot{m}_p h_9}_{\Delta\dot{H}_{D,a}} \tag{8}$$

where $\Delta\dot{H}_{D,w}$ is the total change in enthalpy for the seawater stream and $\Delta\dot{H}_{D,a}$ is the total change in enthalpy of the moist air stream, which includes the exiting condensate

stream.

Second Law.

$$0 = \dot{m}_w \left(s_5 - s_6\right) + \dot{m}_a \left(s_4 - s_1\right) - \dot{m}_p s_9 + \dot{S}_{gen,D} \tag{9}$$

Effectiveness. The dehumidifier effectiveness is found by combining Eqs. (4), (7a) and (8):

$$\epsilon_{D,w} = \frac{h_5 - h_6}{h_5 - h_{i,6}} \qquad \epsilon_{D,a} = \frac{(h_4 - h_1) - (\omega_4 - \omega_1)h_9}{(h_4 - h_{i,1}) - (\omega_4 - \omega_{i,1})h_{i,9}} \tag{10a}$$

$$\epsilon_D = \max\left(\epsilon_{D,w}, \epsilon_{D,a}\right) \tag{10b}$$

Exergy Balance. This can be calculated in two ways — either using the exergy balance directly or from the amount of entropy generated in the component. ξ is specific exergy of the mixture per kilogram of dry air, relative to the dead state.

$$\begin{aligned} \dot{\Xi}_{d,D} &= \dot{m}_w \left(\xi_5 - \xi_6\right) + \dot{m}_a \left(\xi_4 - \xi_1\right) - \dot{m}_p \xi_9 \\ &= T_0 \dot{S}_{gen,D} \end{aligned} \tag{11}$$

Exergetic Efficiency.

$$\eta_{II,D} = 1 - \frac{\dot{\Xi}_{d,D}}{\dot{m}_a \xi_4 + \dot{m}_w \xi_5} \tag{12}$$

Condensate Bulk Temperature. The bulk temperature of the product (condensate) stream can be found by evaluating the following integral, which assumes continuous removal of condensate [13]:

$$\dot{H}_b = \dot{m}_{da} \int_{T_{WB},out}^{T_{WB,in}} h_f(T_{WB}) \left(\frac{d\,\omega}{d\,T_{WB}}\right) d\,T_{WB} \tag{13}$$

Once the bulk enthalpy is known, it can be converted to the specific enthalpy by

dividing through by the mass flow rate of product water. Finally, the bulk temperature can be determined using property tables and the known state variables. Using a least-squares surface fit, it was found that the bulk product temperature is approximately given by the following polynomial function:

$$\begin{aligned} T_p =& 0.0051918 T_{WB,in}^2 + 0.0027692 T_{WB,out}^2 \\ & - 0.007417 T_{WB,in} T_{WB,out} \\ & - 0.41913 T_{WB,in} + 1.0511 T_{WB,out} \\ & + 61.6186 \end{aligned} \tag{14}$$

where all of the temperatures are in kelvin. Equation (14) is valid for $293\,\mathrm{K} \leq T_{WB} \leq 363\,\mathrm{K}$ and has a maximum relative error of less than 0.5%. Note that when the air stream is saturated, the wet-bulb temperature is equivalent to the dry bulb temperature. Calculations were performed in MATLAB [14] and REFPROP [15].

4.3.3. Humidifier

The humidifier is a simple direct contact heat and mass exchanger, essentially a cooling tower. Unlike a cooling tower, where the primary goal is to cool process water, the purpose of the humidifier is to humidify (and heat) the air stream. Since the components work in much the same way, the analyses of a cooling tower and humidifier are identical. The appropriate equations are listed below.

First Law.

$$0 = \underbrace{\dot{m}_a \left(h_2 - h_3\right)}_{\Delta \dot{H}_{H,a}} + \underbrace{\dot{m}_w h_7 - \dot{m}_b h_8}_{\Delta \dot{H}_{H,w}} \tag{15}$$

where $\Delta \dot{H}_{H,w}$ is the total change in enthalpy for the seawater stream and $\Delta \dot{H}_{H,a}$ is the total change in enthalpy of the moist air stream.

Second Law.

$$0 = \dot{m}_a \left(s_2 - s_3\right) + \dot{m}_w s_7 - \dot{m}_b s_8 + \dot{S}_{gen,H} \tag{16}$$

Effectiveness. The humidifier effectiveness is found by combining Eqs. (5), (7a) and (15):

$$\epsilon_{H,w} = \frac{h_7 - (1 - \frac{1}{mr}(\omega_3 - \omega_2))h_8}{h_7 - (1 - \frac{1}{mr}(\omega_{i,3} - \omega_2))h_{i,8}} \qquad \epsilon_{H,a} = \frac{h_2 - h_3}{h_2 - h_{i,3}} \tag{17a}$$

$$\epsilon_H = \max\left(\epsilon_{H,w}, \epsilon_{H,a}\right) \tag{17b}$$

Exergy Balance.

$$\begin{aligned} \dot{\Xi}_{d,H} &= \dot{m}_a \left(\xi_2 - \xi_3\right) + \dot{m}_w \xi_7 - \dot{m}_b \xi_8 \\ &= T_0 \dot{S}_{gen,H} \end{aligned} \tag{18}$$

Exergetic Efficiency.

$$\eta_{II,H} = 1 - \frac{\dot{\Xi}_{d,H}}{\dot{m}_a \xi_2 + \dot{m}_w \xi_7} \tag{19}$$

4.3.4. Air and Water Heaters

First Law. Since the temperature range is not too large (less than 50 K) and the humidity ratio is constant when heating the air stream, the approximation of constant specific heat is reasonable. The specific heat of the stream is evaluated at the average stream temperature.

$$0 = \dot{m}_h c_{p,h} \left(T_{in} - T_{out}\right) + \dot{Q} \tag{20}$$

where the subscript, h, pertains to the stream that is being heated.

Second Law. Unlike the other, adiabatic components, the heater has an entropy transfer that must be evaluated in order to calculate the entropy generation.

$$0 = \dot{m}_h \left(s_{in} - s_{out} \right) + \dot{S}_{trans} + \dot{S}_{gen,HT} \tag{21}$$

The entropy transfer can be calculated by assuming that the stream is heated with a constant linear heat flux, $\dot{Q}/L$ [W/m], and that the wall temperature is greater than that of the bulk stream by a constant ΔT. Based on known results for solar collectors [16], both these approximations are reasonable.

The bulk fluid temperature, as a function of x, is then given by

$$T_b(x) = T_{in} + \frac{\left(\dot{Q}/L\right)}{\dot{m}_h c_{p,h}} x \tag{22}$$

and the wall temperature is:

$$T_{wall}(x) = T_b + \Delta T = (T_{in} + \Delta T) + \frac{\left(\dot{Q}/L\right)}{\dot{m}_h c_{p,h}} x \tag{23}$$

The rate of entropy transfer can then be calculated as follows [5, 17]:

$$\begin{aligned} \dot{S}_{trans} &= \int_0^L \frac{\dot{Q}(x)}{T_{wall}(x)}\, dx \\ &= \dot{m}_h c_{p,h} \log \left[\frac{\dot{Q}}{\dot{m}_h c_{p,h} \left(T_{in} + \Delta T \right)} + 1 \right] \end{aligned} \tag{24}$$

Once the entropy transfer is determined, calculation of entropy generation is performed using the entropy balance.

Exergy Balance. The exergy balance is performed in the same manner as the entropy balance.

$$\dot{\Xi}_{d,HT} = \dot{m}_h \left(\xi_{in} - \xi_{out} \right) + \dot{\Xi}_{trans} \tag{25}$$

Exergy associated with heat transfer can be calculated as follows:

$$\begin{aligned}\dot{\Xi}_{trans} &= \int_0^L \left(1 - \frac{T_0}{T_{wall}(x)}\right) \dot{Q}(x)\, dx \\ &= \dot{Q} - T_0 \dot{S}_{trans}\end{aligned} \tag{26}$$

Once the exergy transferred with the heat transfer process is calculated, calculation of the exergy destruction is performed using the exergy balance.

Exergetic Efficiency.

$$\eta_{II,HT} = 1 - \frac{\dot{\Xi}_{d,HT}}{\dot{m}_h \xi_{in} + \dot{\Xi}_{trans}} \tag{27}$$

4.4. Evaluation of Properties

4.4.1. Fluid Properties

All fluid property data were taken from the commercial software, Engineering Equation Solver (EES) [18]. EES evaluates water properties using the International Association for the Properties of Water and Steam, 1995 Formulation [19]. Air properties are evaluated using the ideal gas formulations presented by Lemmon [20]. Moist air properties are evaluated assuming an ideal mixture of air and steam using the formulations presented by Hyland and Wexler [21]. Moist air properties from EES are in close agreement with the data presented in ASHRAE Fundamentals [22] and pure water properties are equivalent to those found in NIST's property package, REFPROP.

4.4.2. Exergy

The Wepfer approximations [23] were used for evaluating moist air and liquid water exergy:

$$\begin{aligned}\xi_{ma} = &\left(c_{P,a} + \omega c_{P,v}\right) T_0 \left(\frac{T}{T_0} - 1 - \log\frac{T}{T_0}\right) \\ &+ (1+\bar{\omega}) R_{da} T_0 \log\frac{P}{P_0} \\ &+ R_{da} T_0 \left[(1+\bar{\omega})\log\frac{1+\bar{\omega}_0}{1+\bar{\omega}} + \bar{\omega}\log\frac{\bar{\omega}}{\bar{\omega}_0}\right]\end{aligned} \tag{28}$$

$$\begin{aligned}\xi_w \cong &\left[h_f(T) - h_g(T_0)\right] - T_0\left[s_f(T) - s_g(T_0)\right] \\ &+ \left[P - P_{sat}(T)\right] v_f(T) - R_v T_0 \log\phi_0\end{aligned} \tag{29}$$

When performing an exergy analysis of a system, proper selection of the dead state is critical for proper calculations. Since psychrometric processes involve a mixture of dry air and liquid water, it is important to select a single dead state that corresponds to an equilibrium of both substances. For this analysis, the dead state is selected to be moist air at atmospheric conditions: $T_0 = 20\,^{\circ}\mathrm{C}$, $p_0 = 101.325\,\mathrm{kPa}$, and $\phi_0 = 0.6$. The dead state of the water in the system (regardless of phase) is water vapor at the specified temperature, and a pressure equal to the partial pressure of water vapor at the corresponding moist air state specified above.

4.5. Input Conditions

When defining the operating conditions of the cycle, there are two general approaches that can be considered. First, the analysis can be performed assuming a constant production rate with the top temperature fixed ($\dot{m}_p = 1$; fixed T_7 for WH, fixed T_4 for AH). Second, the analysis can be performed assuming a constant energy inflow (constant heat input, $\dot{Q}$ and inlet seawater flow rate, $\dot{m}_w$). Ultimately, at least one mass flow rate (plus mass flow rate ratio, m_r) and either the heat flux or top temperature must be specified for the cycle to be fully defined. Both methods of analysis are considered in this study. In both methods, the component effectiveness is arbitrarily selected. In addition to the specified operating conditions, the environmental

conditions (specifically, the seawater state 5) are known and fixed.

This type of analysis is considered "on-design" since each set of parameters constitutes a different plant rather than an existing plant at various operating conditions. This is because different size components are required to achieve a given effectiveness for different temperatures and flow rates. It is important to keep in mind that each data point presented is a unique plant.

5. Solution Technique and Validation

Due to the complexity of analyzing multi-stream cycles with mixing, EES was used to solve the cycles for various operating conditions. EES automatically identifies and groups equations that must be solved simultaneously and then solves the system iteratively. The default convergence values (maximum residual $< 10^{-6}$; change of variable $< 10^{-9}$) were used in this study as well as in [4, 6, 7]. Additionally, EES has built-in property packages.

The equations for the First Law, mass balances, and component effectiveness presented in Sec. 4, along with the selected input conditions fully define the system. These equations and conditions are used to solve for the remaining unknown temperatures. Once all the system states are known, the Second Law equations, exergy equations, and performance parameters are evaluated.

The component and system models were validated by performing hand calculations to ensure that the results presented were consistent. Additionally, limiting cases such as component effectiveness of zero and one were performed in order to make sure that the model behaved as expected.

In order to further validate the model presented here, the results were compared to the trends observed in the paper by Amer et al. [24]. Amer et al. performed both theoretical and experimental analysis of a CAOW-WH cycle and presented trends of

how various parameters such as temperatures and humidity ratios within the system vary with respect to the system top temperature. It was found that the model presented in the current work followed the same trends seen in Amer's work. For example, the water exit temperature from the dehumidifier and the humidity ratio at the inlet and outlet of the dehumidifier all increase with increasing cycle top temperature.

6. Results

6.1. Minimizing Specific Entropy Generation Maximizes GOR

A previous study [4] has shown that GOR is a strong function of mass flow rate ratio, component effectivenesses, and system top temperatures (or heat flow rates). Therefore, this study looks at the same parameters but also closely considers the entropy generation in each cycle. Note that the kinks in the following graphs correspond to points where the definition of component effectiveness switches as a result of the `max()` function in Eq. (7b).

Figure 2 shows GOR (solid lines) and the specific entropy generation (dashed lines) as a function of m_r for a CAOW-WH cycle with a fixed top temperature and varying component effectiveness. Specific entropy generation is defined as the cycle's total entropy generation divided by the mass flow rate of the product stream (condensate). Similarly, Fig. 3 shows the same quantities for a WH cycle in which the component effectivenesses are fixed and the amount of heat input is varied. Figure 4 plots the same values for an AH cycle with fixed component effectiveness and varying top temperature.

[Figure 2 about here.]

[Figure 3 about here.]

[Figure 4 about here.]

The first immediately visible result is that peak GOR corresponds to minimum specific entropy generation for both cycles, and regardless of the operating conditions. That is, for each cycle, there is an optimal configuration that both minimizes entropy generation and maximizes GOR. By optimizing a cycle for minimum specific entropy generation, the cycle is also optimized for maximum GOR.

This trend is not present when comparing GOR to the total entropy generation for the system rather than the specific entropy generation. Figure 5 illustrates an example of GOR increasing with increasing *total* entropy generation for the same cycle configuration used to create Fig. 3. Note that GOR is not a single valued function of either total entropy generation or specific entropy generation. This is because GOR was evaluated by varying the mass flow rate ratio as seen in Figs. 2–3.

[Figure 5 about here.]

If the data from Fig. 5 is instead replotted versus the specific entropy generation (Fig. 6), it is seen that as the specific irreversibilities within the cycle decrease, the performance of the system increases. This is a satisfying result since it matches the fact that performance should improve with decreasing irreversibility. Furthermore, it is also in line with the ideal heat of separation calculation given in the appendix.

[Figure 6 about here.]

This trend of increasing GOR with decreasing specific entropy generation was present for all the cycle types and configurations analyzed in this paper. Figure 7 shows a plot of GOR versus specific entropy generation for several cases of both the air and water heated cycles. The cases presented in this figure are listed in Table 1. In each case, the component effectivenesses and either the top temperature or the heat input was held constant while the mass flow rate ratio was varied.

[Figure 7 about here.]

Note that in Fig. 7, the curves do not collapse to a single curve and that knowing GOR is not sufficient for determining the entropy generation (and vice versa). Instead, for a fixed GOR, it is easy to see that there are several cycles that have the same performance but with different amounts of entropy generated. From a cost point of view, the "best" cycle is likely to be the one with the maximum entropy generation since this will imply higher irreversibilities, and therefore, a smaller system size. Fakheri discusses how in a heat exchanger, minimum entropy generation is not the end goal since a completely reversible exchanger would have to be infinitely large [25]. While Fakheri only looked at heat exchangers, this concept applies to heat and mass exchangers as well [12].

At first, this seems to be a paradox — maximizing GOR minimizes entropy generation, but the maximum entropy generation is desired. At this point, it is important to make a distinction between operating conditions and cycles. For a given cycle, minimizing entropy generation will maximize GOR. However, when comparing different cycles, the cycle that has the highest entropy generation for a given GOR is likely to be the economically ideal case.

[Table 1 about here.]

6.2. Identification of Limiting Components

In the basic CAOW HD cycles, either the humidifier or the dehumidifier will limit the performance of the overall system. The performance limit is a result of a minimum temperature pinch within the particular component. Further improvements in effectiveness are not possible since it would result in negative entropy generation (i.e., a temperature cross within the exchanger).

Identification of the limiting component is simple when looking at the specific entropy generation in each of the components of the cycle. As with the total specific entropy generation of the cycle defined in Eq. (2), entropy generation within each component is normalized to the mass flow rate of the product stream. Figure 8 shows the specific entropy generation within each component of a CAOW-WH cycle with fixed top temperature as a function of the mass flow rate ratio. GOR is also plotted on the second axis for comparison. This figure presents a few key concepts. First, the specific entropy generation within the dehumidifier, humidifier, and heater are all of the same order of magnitude, which means that all of the components must be studied carefully when designing the system. Second, maximum GOR does not occur at a point where all of the components have minimum entropy generation, but rather, where the total specific entropy generation of the system is minimum (in this figure, the amount of water produced is constant so a plot of specific entropy generation would be a scaled version of total entropy generation). Third, one of the components tends toward zero entropy generation (in this case, the humidifier) in which case it cannot be further improved to have a greater effectiveness. For this particular cycle, the designer should concentrate on improving the effectiveness of the dehumidifier in order to improve the overall performance of the system.

[Figure 8 about here.]

Figure 9 plots specific entropy generation within the components of a CAOW-AH cycle with fixed top temperature. For this particular cycle, it is clear that the limiting component depends on the mass flow rate ratio. Focusing on the humidifier and dehumidifier, it is seen that for $m_r < 1.56$, entropy generation in the dehumidifier is less than the production within the humidifier and vice versa for $m_r > 1.56$. When trying to maximize GOR, however, entropy generation in the dehumidifier quickly tends to-

ward zero indicating a pinch constraint. Therefore, the effectiveness of the dehumidifier cannot be further increased and the designer should focus on improving the humidifier.

[Figure 9 about here.]

As seen in Fig. 9, the limiting component may switch depending on operating conditions. By looking at the entropy generation of each component of the cycle, the designer can quickly determine which component should be the focus of the design effort for given operating conditions. This method of entropy generation analysis can be used for both on- and off-design assessments. During on-design work, it is easy to identify which component will require more attention, while during off-design work it is easy to see which component should be renovated, modified, or otherwise improved. Evaluating the entropy generation is much simpler than performing a full pinch analysis, e.g. as done by Hou [26]. Once the limiting component has been determined, use of pinch analysis can further aid the design process and allow for proper design and optimization of the complete HD system.

6.3. Exergetic Efficiency

Some authors have suggested using exergy for analysis of HD systems [27, 28]. However, in this work, it was found that there is no consistent correlation between a cycle's exergetic efficiency and GOR. It is again important to note that all of the analysis done in this paper is on-design, that is, a cycle is being selected for best performance rather than trying to optimize an existing plant to the best operating conditions. Since each set of conditions corresponds to a different plant, exergy analysis did not prove as useful as one would initially expect.

A thought experiment helps to illustrate this point. From Eq. 3, it is clear that there are at least two cases in which η_{II} will be zero — when there is no interaction between streams (i.e., nothing happens) and when the amount of exergy input is much greater

than the exergy destruction. The second case can be illustrated using the CAOW-WH cycle. As the mass flow rate of seawater increases toward infinity, the amount of exergy entering the system also tends toward infinity. Likewise, the amount of heat required to heat the water stream goes to infinity. Since the seawater stream has a near infinite heat capacity, the humidifier and dehumidifier behave similar to single stream heat exchangers (only one stream is changing temperature) which means the exergy destruction is finite and based on the amount of air in the system. Even though the flow rate of seawater is large, the amount of product produced is limited by the amount of air in the system which means there is a finite amount of water production. Therefore, GOR is very small (small mass production, large heat input), and η_{II} is very close to one since the large exergy input will greatly dominate the finite exergy destruction.

[Figure 10 about here.]

When taking these two limiting cases into account, it is clear that exergetic efficiency will not yield conclusive results for the design of a high GOR HD cycle. Additionally, the appendix discusses thermodynamic arguments suggesting that η_{II} should not be expected to fully capture the effects of irreversibility in these cycles. Figure 10 plots GOR versus Second Law efficiency of several CAOW cycles under the operating conditions listed in Table 1. The lack of a general trend in this figure supports the conclusion that Second Law efficiency is not an appropriate tool for on-design analysis of CAOW HD cycles. Once an actual plant has been designed, however, it is believed that using Second Law efficiency to further improve the existing plant will be effective.

7. Conclusions

Entropy generation minimization analysis has helped to identify the key components and operating conditions that should be considered while designing heating dehumidi-

fication systems. In this regard, the following conclusions can be summarized:

1. For a given cycle, there is a specific mass flow rate ratio that simultaneously minimizes specific entropy generation and maximizes GOR. This shows that minimizing specific irreversibility leads to peak performance.
2. In any given cycle, the effectiveness of either the humidifier or dehumidifier will be limited by the system's minimum temperature pinch. A designer should focus on improving the other component in order to reduce the total irreversibilities within the system.
3. Exergetic efficiency fails to provide meaningful insight into the optimization of the basic HD cycles when studying from an on-design point of view.

Acknowledgments

The authors would like to thank the King Fahd University of Petroleum and Minerals for funding the research reported in this paper through the Center for Clean Water and Clean Energy at MIT and KFUPM.

Appendix: Heat of Separation

Figure 11 shows a black-box thermal desalination system. Since the air never leaves the system boundary in a CAOW cycle, the least work of separation should be independent of air flow rate.

In the following section, $\bar{x}$ is a property of the mixture per mol, $\bar{x}_i$ is the partial molar property of species i, and $\dot{n}_i$ is the molar flow rate of species i. The heat of separation is denoted by $\dot{Q}_{sep}$. State 1 is the incoming seawater, state 2 is pure water (product), and state 3 is the concentrated brine, all at T_0.

[Figure 11 about here.]

Heat of Separation:

First and Second Law for black-box HD system:

$$\begin{aligned} \dot{Q}_{sep} + \left(\dot{n}\bar{h}\right)_1 &= \left(\dot{n}\bar{h}\right)_2 + \left(\dot{n}\bar{h}\right)_3 \quad (30) \\ \frac{\dot{Q}_{sep}}{T_H} + \left(\dot{n}\bar{s}\right)_1 + \dot{S}_{gen} &= \left(\dot{n}\bar{s}\right)_2 + \left(\dot{n}\bar{s}\right)_3 \quad (31) \end{aligned}$$

Multiply Eq. (31) by inlet/outlet temperature, T_0 and subtract from Eq. (30).

$$\begin{aligned} \dot{Q}_{sep} - \frac{T_0}{T_H}\dot{Q}_{sep} + \dot{n}_1\left(\bar{h} - T_0\bar{s}\right)_1 - T_0\dot{S}_{gen} \\ = \dot{n}_2\left(\bar{h} - T_0\bar{s}\right)_2 + \dot{n}_3\left(\bar{h} - T_0\bar{s}\right)_3 \end{aligned} \quad (32)$$

Since enthalpy and entropy for all three streams is evaluated at T_0, the Gibbs free energy can be written as, $\bar{g} = \bar{h} - T_0\bar{s}$.

$$\left(1 - \frac{T_0}{T_H}\right)\dot{Q}_{sep} = \dot{n}_2\bar{g}_2 + \dot{n}_3\bar{g}_3 - \dot{n}_1\bar{g}_1 + T_0\dot{S}_{gen} \quad (33)$$

Now, define the recovery ratio and mole ratio of salt in the seawater as:

$$\begin{aligned} R_p &\equiv \frac{\dot{n}_{H_2O,2}}{\dot{n}_{H_2O,1}} = \frac{\text{Product Water}}{\text{Inlet Seawater}} \\ \eta &\equiv \frac{\dot{n}_{NaCl,1}}{\dot{n}_{H_2O,1}} = \frac{\text{mol salt in seawater}}{\text{mol water in seawater}} \end{aligned}$$

The Gibbs free energy of the mixture per mol, $\bar{g}$, can be rewritten in terms of the partial molar properties, $\dot{n}\bar{g} = \left(\dot{n}\bar{g}\right)_{H_2O} + \left(\dot{n}\bar{g}\right)_{NaCl}$. Rewriting Eq. (33) in terms of the partial molar properties and dividing through by the molar flow rate of seawater,

$\dot{n}_{H_2O,1}$, gives the following expression:

$$\begin{aligned}\frac{\dot{Q}_{sep}}{\dot{n}_{H_2O,1}} =& \left(1-\frac{T_0}{T_H}\right)^{-1}\Big[\eta\left(\bar{g}_{NaCl,3}-\bar{g}_{NaCl,1}\right)\\ &+\left(\bar{g}_{H_2O,3}-\bar{g}_{H_2O,1}\right)\\ &+R_p\left(\bar{g}_{H_2O,2}-\bar{g}_{H_2O,3}\right)\Big]\\ &+\frac{T_0}{\left(1-\frac{T_0}{T_H}\right)}\frac{\dot{S}_{gen}}{\dot{n}_{H_2O,1}}\end{aligned} \tag{34}$$

The bracketed term in Eq. (34) is known as the least work of separation per mole of seawater entering, $\dot{W}_{least}/\dot{n}_{H_2O,1}$.

$$\frac{\dot{Q}_{sep}}{\dot{n}_{H_2O,1}} = \frac{\dot{W}_{least}\left(\Delta\bar{g}_{H_2O},\Delta\bar{g}_{NaCl}\right)}{\left(1-\frac{T_0}{T_H}\right)\dot{n}_{H_2O,1}} + \frac{T_0}{\left(1-\frac{T_0}{T_H}\right)}\frac{\dot{S}_{gen}}{\dot{n}_{H_2O,1}} \tag{35}$$

Finally, the above expression can be converted to heat input per unit mass of water produced by multiplying by $(1/R_p)(1000/MW_{H_2O})$, where MW_{H_2O} is the molecular weight of water:

$$\frac{\dot{Q}_{sep}}{\dot{m}_p} = \frac{\dot{W}_{least}\left(\Delta\bar{g}_{H_2O},\Delta\bar{g}_{NaCl}\right)}{\left(1-\frac{T_0}{T_H}\right)\dot{m}_p} + \frac{T_0}{1-\frac{T_0}{T_H}}\left(\frac{\dot{S}_{gen}}{\dot{m}_p}\right) \tag{36}$$

In this above equation, it is noted that $\dot{Q}_{sep}/\dot{m}_p$ is the same grouping of parameters that is seen in GOR, Eq. (1). This calculation suggests that to maximize GOR, the right hand side of the equation must be minimized. Since the least heat of separation should not change significantly when varying the cycle conditions (compared to the heat input in the real case), it is seen that minimizing $\dot{S}_{gen}/\dot{m}_p$ should maximize GOR.

When trying to determine the limiting components as in Sec. 6.2, specific entropy generation in each component is examined. This is defined as the entropy generated

in the component divided by the system's product flow rate, $\dot{m}_p$. This is a suitable parameter since optimum system performance, rather than individual component performance, is desired.

A term that resembles total exergy destruction, $T_0\dot{S}_{gen}$, is also present in Eq. (36). However, note that T_0 represents the temperature of the three fluid streams, not the dead state temperature, and therefore, exergy destruction does not explicitly appear in Eq. (36).

Since it is seen that minimizing the specific entropy generation leads to maximum GOR and since total exergy destruction is directly related to the total entropy generation, one might expect that maximizing exergetic efficiency would similarly lead to maximum GOR. However, Eq. (36) shows that GOR is a function of the flow rate of the product stream whereas it is seen in Eq. (3) that the exergetic efficiency, η_{II}, is not a function of $\dot{m}_p$. Therefore, it should not be expected that η_{II} will fully capture the effects of irreversibilities in CAOW HD cycles.

References

[1] S. Parekh, M. M. Farid, J. R. Selman, S. Al-hallaj, Solar desalination with a humidification-dehumidification technique — a comprehensive technical review, Desalination 160 (2) (2004) 167–186.

[2] E. Chafik, Design of plants for solar desalination using the multi-stage heating/humidifying technique, Desalination 168 (2004) 55–71, Desalination Strategies in South Mediterranean Countries.

[3] G. P. Narayan, M. H. Sharqawy, E. K. Summers, J. H. Lienhard V, S. M. Zubair, M. Antar, The potential of solar-driven humidification-dehumidification desalination for small-scale decentralized water production, Renewable and Sustainable Energy Reviews 14 (4) (2010) 1187–1201.

[4] G. P. Narayan, M. H. Sharqawy, J. H. Lienhard V, S. M. Zubair, Thermodynamic analysis of humidification dehumidification desalination cycles, Desalination and Water Treatment 16 (2010) 339–353.

[5] A. Bejan, Advanced Engineering Thermodynamics, 3rd Edition, John Wiley & Sons, Inc., Hoboken, New Jersey, 2006.

[6] B. A. Qureshi, S. M. Zubair, Application of exergy analysis to various psychrometric processes, Journal of Energy Research 27 (2003) 1079–1084.

[7] B. A. Qureshi, S. M. Zubair, Second-law-based performance evaluation of cooling towers and evaporative heat exchangers, International Journal of Thermal Sciences 46 (2) (2007) 188–198.

[8] S. Eftekharzadeh, M. M. Baasiri, P. A. Lindahl Jr., Feasibility of seawater cooling

towers for large-scale petrochemical development, Tech. Rep. TP03-17, Cooling Technology Institute, San Antonio, Texas (February 2003).

[9] M. H. Sharqawy, J. H. Lienhard V, S. M. Zubair, Thermophysical properties of seawater: A review of existing correlations and data, Desalination and Water Treatment 16 (2010) 354–380.

[10] M. H. Sharqawy, J. H. Lienhard V, S. M. Zubair, On thermal peroformance of seawater cooling towers, in: Proceedings of the International Heat Transfer Conference IHTC14, no. 23200, International Heat Transfer Conference, Washington DC, USA, August 8–13, 2010, accepted.

[11] G. P. Narayan, K. H. Mistry, M. H. Sharqawy, S. M. Zubair, J. H. Lienhard V, Energy effectiveness of simultaneous heat and mass exchange devices, Frontiers in Heat and Mass Transfer, Accepted for publication (May 2010) 1 (2).

[12] G. P. Narayan, J. H. Lienhard V, S. M. Zubair, Entropy generation minimization of combined heat and mass transfer devices, International Journal of Thermal Sciences, Accepted for Publication (April 2010).

[13] K. H. Mistry, Second Law Analysis and Optimization of Humidification-Dehumidification Desalination Cycles, Master's thesis, Massachusetts Institute of Technology, Cambridge, MA (June 2010).

[14] The MathWorks, MATLAB R2008A (February 2008).
URL `http://www.mathworks.com/`

[15] E. W. Lemmon, M. L. Huber, M. O. McLinden, NIST Standard Reference Database 23: Reference Fluid Thermodynamic and Transport Properties-REFPROP, Version 8.0 (2007).

[16] J. A. Duffie, W. A. Beckman, Solar Engineering of Thermal Processes, 3rd Edition, John Wiley & Sons, Inc., Hoboken, New Jersey, 2006.

[17] M. J. Moran, H. N. Shapiro, Fundamentals of Engineering Thermodynamics, 6th Edition, John Wiley & Sons, Inc., New Jersey, 2007.

[18] S. A. Klein, Engineering Equation Solver, Academic Professional, Version 8. URL `http://www.fchart.com/`

[19] W. Wagner, A. Pruss, The IAPWS Formulation 1995 for the Thermodynamic Properties of Ordinary Water Substance for General and Scientific Use, Journal of Physical and Chemical Reference Data 31 (2) (2002) 387–535.

[20] E. W. Lemmon, R. T. Jacobsen, S. G. Penoncello, D. G. Friend, Thermodynamic Properties of Air and Mixtures of Nitrogen, Argon, and Oxygen From 60 to 2000 K at Pressures to 2000 MPa, Journal of Physical and Chemical Reference Data 29 (3) (2000) 331–385.

[21] R. W. Hyland, A. Wexler, Formulations for the Thermodynamic Properties of the Saturated Phases of H2O from 173.15 K to 473.15 K, ASHRAE Transactions Part 2A (RP-216) (2793) (1983a) 500–519.

[22] D. J. Wessel, ed., ASHRAE Fundamentals Handbook 2001 (SI Edition), American Society of Heating, Refrigerating, and Air-Conditioning Engineers, 2001.

[23] W. J. Wepfer, R. A. Gaggioli, E. F. Obert, Proper Evaluation of Available Energy for HVAC, ASHRAE Transactions 85(I) (1979) 214–230.

[24] E. Amer, H. Kotb, G. Mostafa, A. El-Ghalban, Theoretical and experimental investigation of humidification-dehumidification desalination unit, Desalination 249 (3) (2009) 949–959.

[25] A. Fakheri, On application of the second law to heat exchangers, in: Proceedings of IMECE2008, no. IMECE2008-69056, International Mechanical Engineering Congress and Exposition, ASME, Boston, Massachusetts, USA, 2008, pp. 501–506.

[26] S. Hou, Two-stage solar multi-effect humidification dehumidification desalination process plotted from pinch analysis, Desalination 222 (1-3) (2008) 572–578, European Desalination Society and Center for Research and Technology Hellas (CERTH), Sani Resort 22–25 April 2007, Halkidiki, Greece.

[27] K. S. Spiegler, Y. M. El-Sayed, The energetics of desalination processes, Desalination 134 (1-3) (2001) 109–128.

[28] S. Hou, D. Zeng, S. Ye, H. Zhang, Exergy analysis of the solar multi-effect humidification-dehumidification desalination process, Desalination 203 (1-3) (2007) 403–409, EuroMed 2006 — Conference on Desalination Strategies in South Mediterranean Countries.

List of Figures

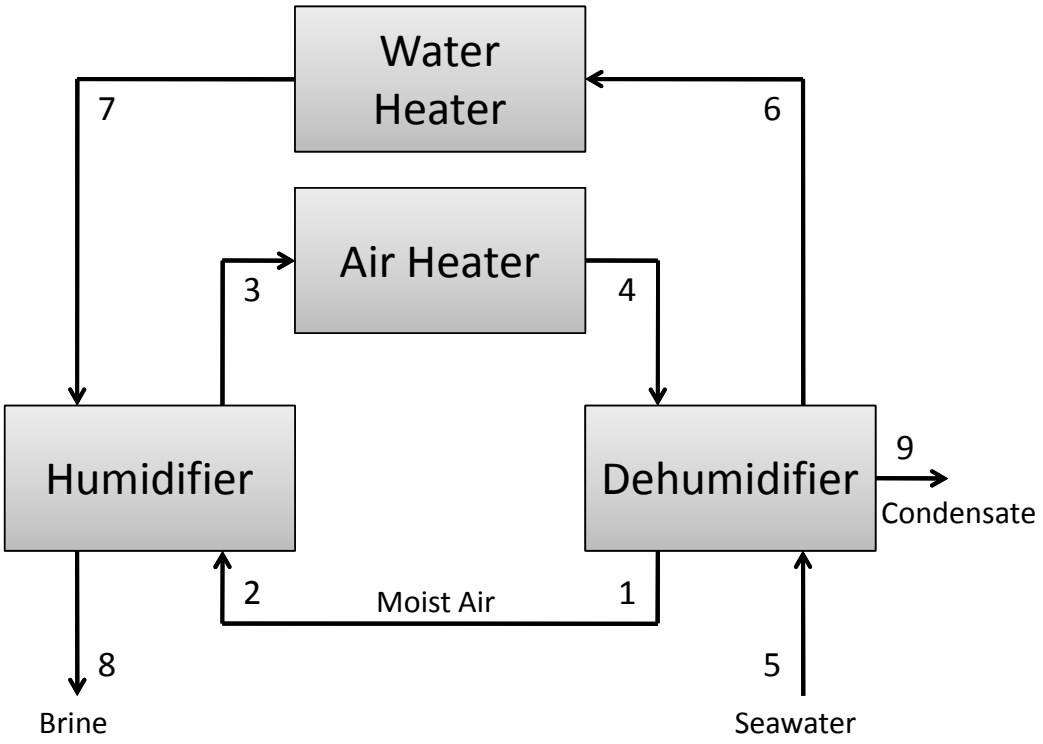

Figure 1: A basic closed air, open water HD cycle with both a water and air heater. Typically, only one heater is used forming either the CAOW-WH or CAOW-AH cycle.

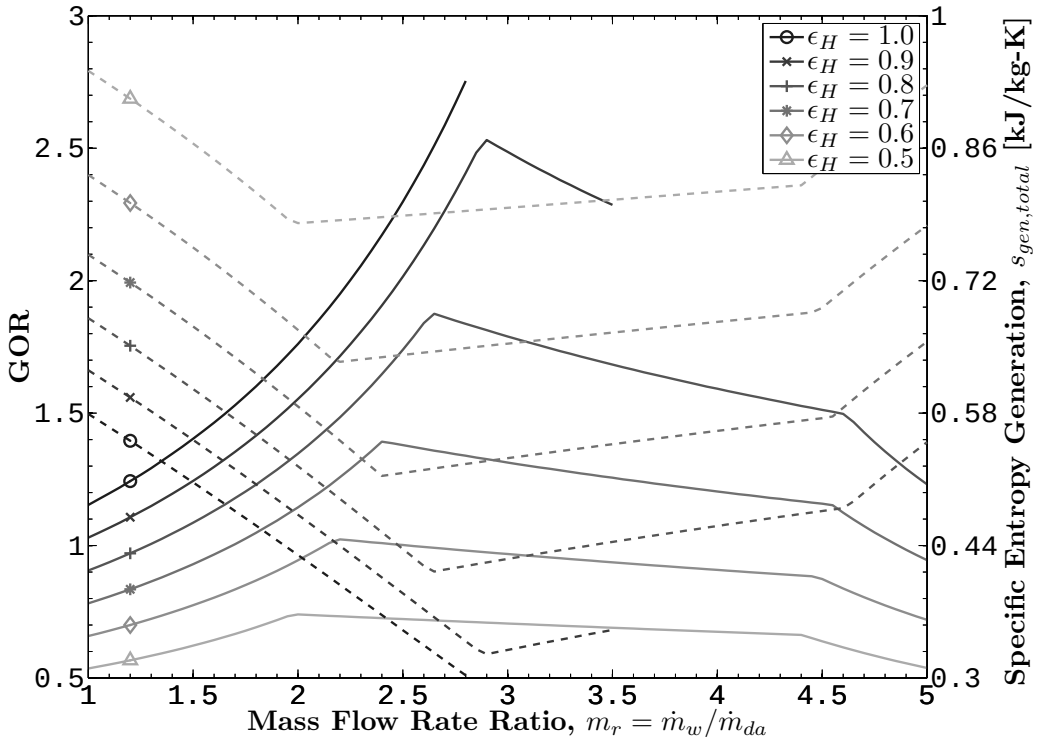

Figure 2: GOR (solid lines) and specific entropy generation (dashed lines) as a function of mass flow rate ratio for a CAOW-WH cycle with $T_{top} = 70\,^{\circ}\mathrm{C}$ and $\epsilon_D = 0.9$.

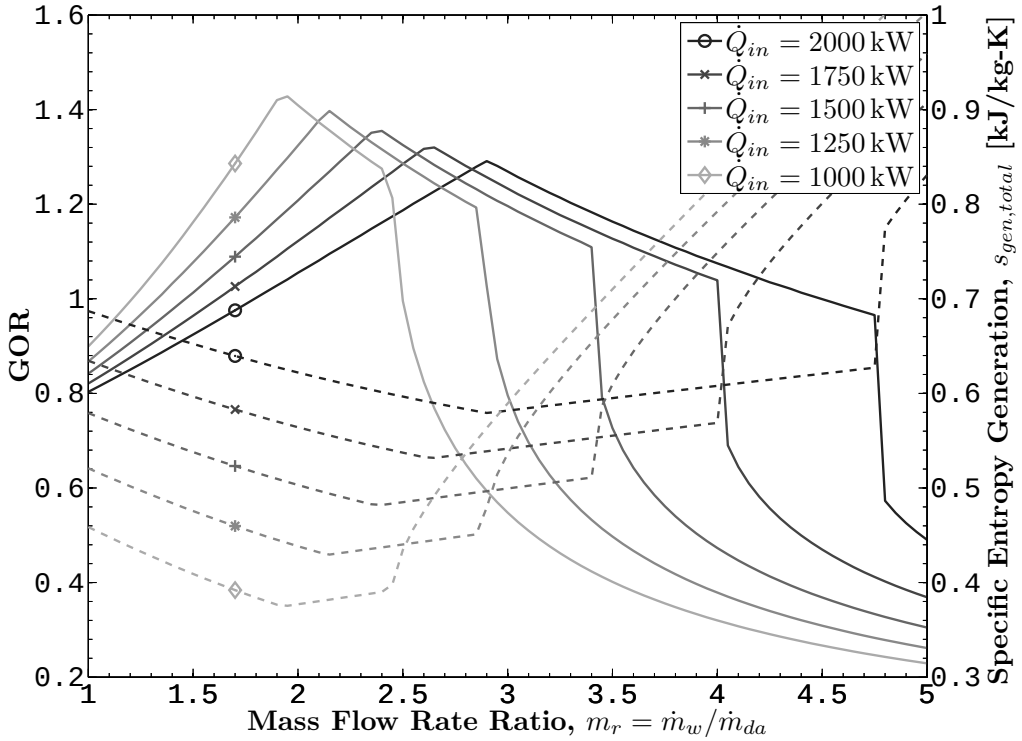

Figure 3: GOR (solid lines) and specific entropy generation (dashed lines) as a function of mass flow rate ratio for a CAOW-WH cycle with fixed energy input and $\epsilon_D = \epsilon_H = 0.8$.

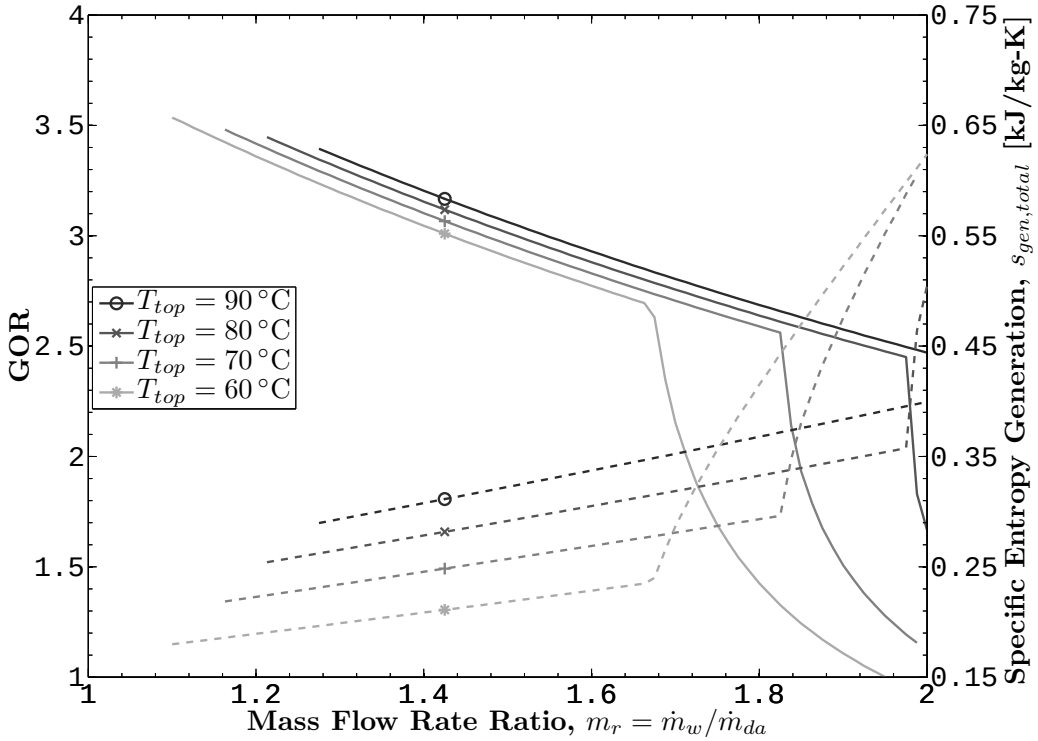

Figure 4: GOR (solid lines) and specific entropy generation (dashed lines) as a function of mass flow rate ratio for a CAOW-AH cycle with $\epsilon_D = \epsilon_H = 0.9$.

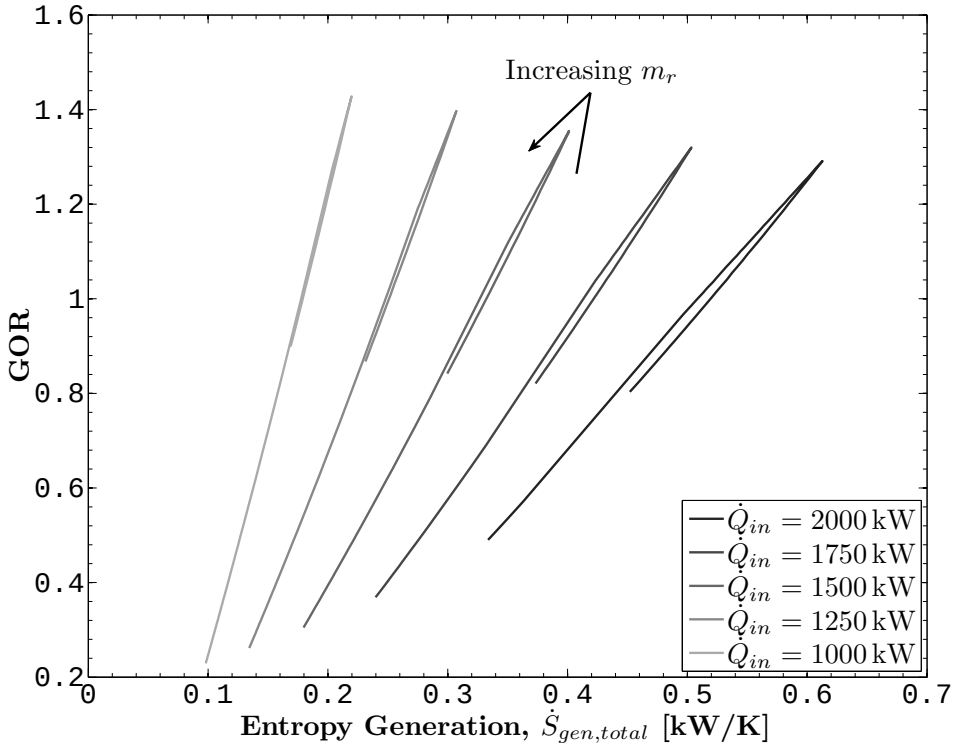

Figure 5: GOR versus total entropy generation, evaluated by varying m_r, for a CAOW-WH cycle with fixed energy input and $\epsilon_D = \epsilon_H = 0.8$.

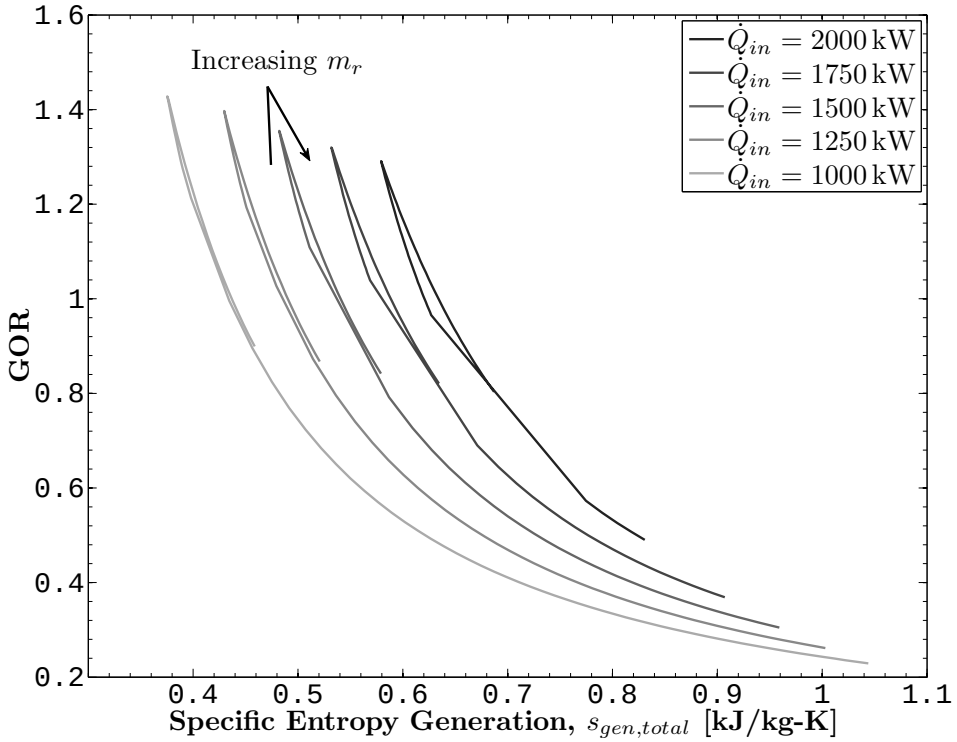

Figure 6: GOR versus specific entropy generation, evaluated by varying m_r, for a CAOW-WH cycle with fixed energy input and $\epsilon_D = \epsilon_H = 0.8$.

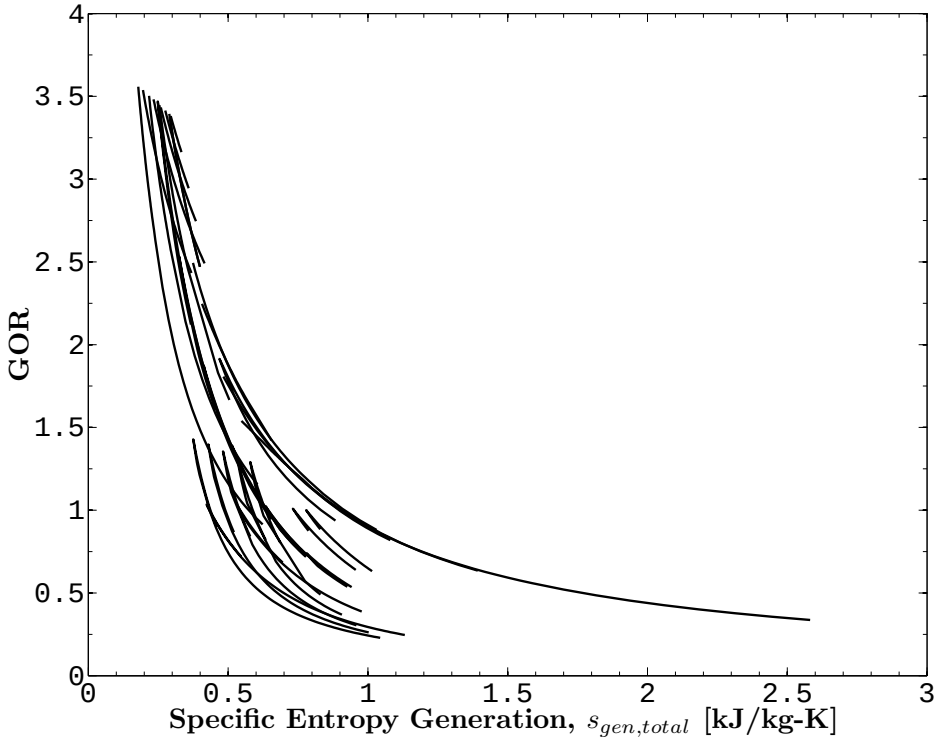

Figure 7: GOR versus specific entropy generation for various CAOW cycle configurations and operating conditions listed in Table 1.

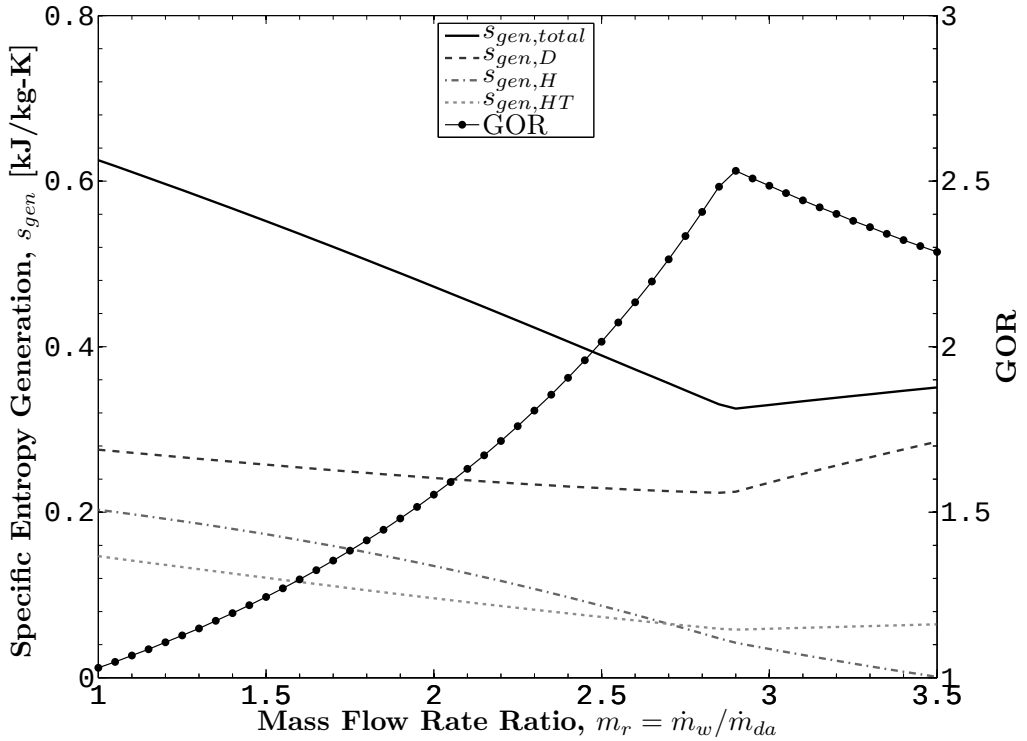

Figure 8: Specific entropy generation within each component of a CAOW-WH cycle with $T_{top} = 70\,^{\circ}\mathrm{C}$ and $\epsilon_D = \epsilon_H = 0.9$.

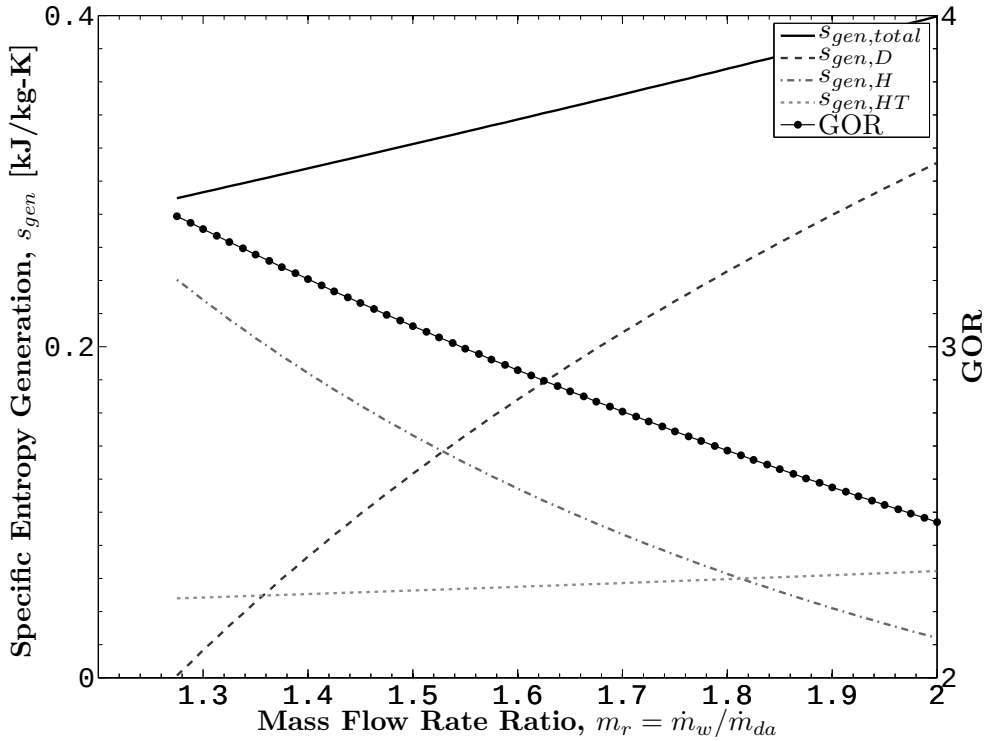

Figure 9: Specific entropy generation within each component of a CAOW-AH cycle with $T_{top} = 90\,^{\circ}\mathrm{C}$ and $\epsilon_D = \epsilon_H = 0.9$.

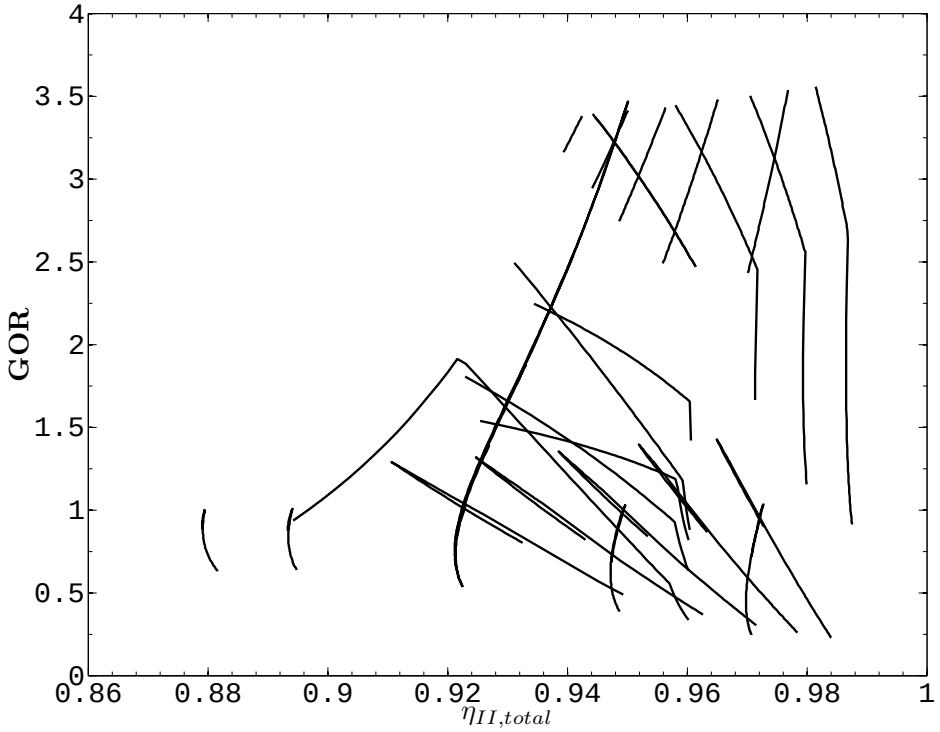

Figure 10: GOR versus Second Law efficiency for CAOW cycle configurations and operating conditions listed in Table 1.

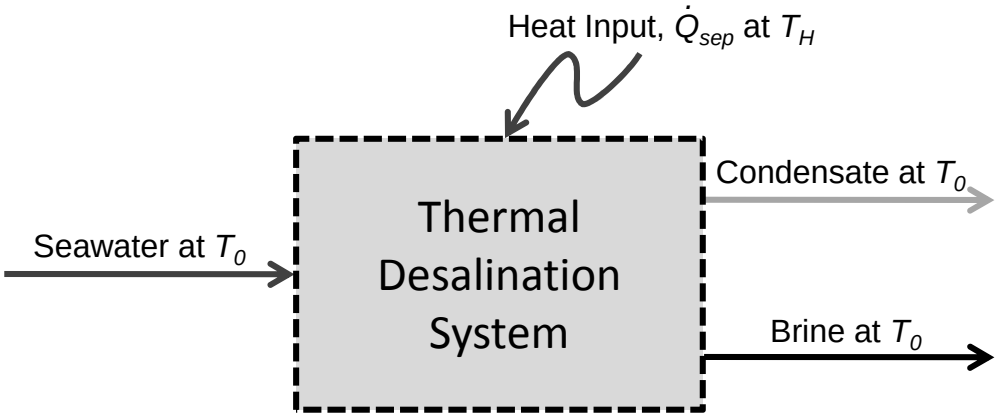

Figure 11: Black-box thermal desalination system with states 1–3 at T_0. State 1: Incoming seawater. State 2: Product water. State 3: Brine. $\dot{Q}_{sep}$ is entering the system at T_H.

List of Tables

Table 1: List of Cycle Types and Configurations

Cycle Type	Constant Parameter	Cases
CAOW-AH	$\epsilon_D = \epsilon_H = 0.9$	$\dot{Q}_{in} = 500, 650, 750, 820, 900\,\mathrm{kW}$
CAOW-AH	$\epsilon_D = \epsilon_H = 0.9$	$T_{top} = 60, 70, 80, 90\,^\circ\mathrm{C}$
CAOW-AH	$T_{top} = 90\,^\circ\mathrm{C}$	ϵ_D, $\epsilon_H = 0.8, 0.7, 0.9$
CAOW-WH	$\epsilon_D = \epsilon_H = 0.8$	$\dot{Q}_{in} = 1000, 1250, 1500, 1750, 2000\,\mathrm{kW}$
CAOW-WH	$\epsilon_D = 0.9$, $\epsilon_H = 0.6$	$T_{top} = 40, 50, 60, 70, 80, 85\,^\circ\mathrm{C}$
CAOW-WH	$T_{top} = 70\,^\circ\mathrm{C}$	$\epsilon_D = 0.9$, $\epsilon_H = 0.5$–1.0